IEEE Access
Multidisciplinary | Rapid Review | Open Access Journal

Received January 25, 2020, accepted February 7, 2020, date of publication February 18, 2020, date of current version February 28, 2020.

Digital Object Identifier 10.1109/ACCESS.2020.2974815

Compact Collinear Quasi-Yagi Antenna Array for Wireless Energy Harvesting

YI-YAO HU, (Student Member, IEEE), SHENG SUN, (Senior Member, IEEE), AND HAO XU
School of Electronic Science and Engineering, University of Electronic Science and Technology of China, Chengdu 611731, China

Corresponding author: Sheng Sun (sunsheng@ieee.org)

This work was supported in part by the National Natural Science Foundation of China under Grant 61622106, Grant 61721001, and Grant 61971115, and in part by the Sichuan Science and Technology Program under Grant 2018RZ0142.

ABSTRACT A novel quasi-Yagi antenna array with a thin configuration is proposed in this work. Different from traditional high-gain Yagi or quasi-Yagi antennas, which need large widths to hold either several parasitic elements along the radiation direction or extra feeding networks like baluns and power dividers, this design adopts a collinear antenna as the driven part and employs a few collinear parasitic strips. Thus, a high gain can be realized with a narrow width. Based on the analysis of the collinear antenna, effect of parasitic strips and impedance matching, a compact antenna prototype with a size of 26 mm $\times$ 190.5 mm is proposed and fabricated. The measured results show that the realized gain is 8–8.7 dBi from 2.3 to 2.63 GHz. With a rectifying circuit, maximum dc power of 1–39.2 μW can be produced under a power density of 0.05–1 μW/cm^2 at 2.45 GHz, while more than 31 μW obtained in an azimuth angle range of 100° for a power density of 1 μW/cm^2. To further validate the compactness, an angle-diversity prototype consisting of two back-to-back proposed array antennas is also presented. It nearly doubles the harvesting coverage with a size less than that of two antennas.

INDEX TERMS Collinear antenna, rectenna, wireless energy harvesting, Yagi-Uda.

I. INTRODUCTION

The size or volume is always a concern in antenna designs, since miniaturization means less cost and occupied space. For portable communication devices, folding or meandering the antenna structure is a common miniaturization technique. Similarly, for the same purpose, folded or meandered dipole, monopole and loop antennas were adopted in rectenna (rectifying antenna) designs [1]–[7]. They are fit for small and limited space at the cost of very low antenna gains. To ensure an enough supply of energy under low power densities, the size or aperture of the antenna part has to be enlarged.

There are two techniques in the process. One emphasizes dc power combining and pursues omnidirectional harvesting patterns. The corresponding design makes the aperture less focused, where multiple antennas with wide beams and low gains separately collect wireless power [8]–[10]. RF power received by each antenna is rectified respectively, and then combined in a form of voltage or current summing. The dc output is elevated by gathering multiple rectennas, or forming a rectenna array. Such designs could capture incident RF energy from different directions due to the wide beams. One issue should be noticed, that the sensitivity of rectifiers to weak RF power is notably low. Unlike communication receivers, which can even receive signals of power levels less than -90 dBm, most rectifiers can provide only a few percent efficiency at -30 dBm around 2.45 GHz, and the rectification efficiency markedly declines when input RF power decreases from -10 dBm [11], [12]. Facing the low power density of ambient RF energy, a low-gain antenna usually cannot supply a rectifying circuit with high RF power, which will necessarily depress the rectification efficiency. Consequently, harvesting performance becomes inefficient since a considerable proportion of energy is wasted in circuits, and the utilization of the enlarged size is lowered. Then the harvesting system will be restricted to locations with relatively high power densities or closer to the power source.

On the contrary, the other technique makes the antenna aperture more focus on one direction and enhances the gain [9], [13]–[19]. In this case, higher RF power can be delivered to a rectifying circuit to raise its conversion efficiency. It reduces the power waste in circuits at the sacrifice of the beam width and spatial coverage. However, with the efficiency limit of commonly used rectifying devices, high

The associate editor coordinating the review of this manuscript and approving it for publication was Muhammad Khandaker.

antenna gains are a prerequisite for effectively harvesting energy of low densities. And a latest research that analyzed and measured WiFi energy harvesting in an indoor environment pointed out that, with multipath propagation and one or more power transmitters, an antenna with a high-gain narrow beam is more likely to succeed in collecting a relatively high level of power than one with a low-gain wide beam [20].

Recently, designs with consideration of both the antenna gain and spatial coverage have been presented [21]–[29]. In [21], [22], the beamforming network was employed to make a patch antenna array with several high-gain beams directed at different angles, and each beam with a maximum gain of about 7–10 dBi was generated by the whole aperture through RF combing. Similarly, the traveling-wave grid-array antenna without beamforming networks is designed to provide two or four symmetrically titled high-gain (11–15.5-dBi) beams [23], [24]. RF power collected by different beams was separately rectified and the produced dc power then combined. Thus, they can compensate for the loss of coverage induced by narrowed beams and raised gains, and improve the utilization of the enlarged size. However, one directional antenna or antenna array cannot overcome itself blind areas. For complementing the coverage and losing less energy in the blind spot, multiple patch or Yagi antennas situated on a cubic [26], [27] or cylindrical structure [22], or placed in a circle [28], [29] or back-to-back patterns [25] were designed and demonstrated. One patch antenna was deployed on one side of the cubic in [27]. For enhancing the harvesting performance, the patch was replaced by the Yagi on the cubic structure [26]. The gain was further elevated to over 8 dBi by using a suspended large patch antenna [25] or a patch antenna array [22].

In this scenario, compactness should be interpreted as high space utilization—how to realize a high gain in a cost-effective way, rather than simply a small or tiny size. Till now, several types of antennas have been presented for high-gain rectenna designs, such as grid array [23], [24], patch array [13], [14], [21], [22], large patch [15], [25], suspended or stacked structure [13], [16], [21], [23]–[25] and Yagi antennas [17]–[19], [28], [29]. In general, as discussed in and reflected by the previous works [17], [18], [23], [26], the endfire Yagi or quasi-Yagi antenna can own the highest ratio of the gain to electrical size. In addition, it can also easily realize a wide frequency band with a planar structure [19], while the patch antenna, the other commonly-used high-gain type, usually requires a very thick suspended configuration. Therefore, it can be more competitive compared to other high-gain antennas. A disadvantage of the Yagi antenna is the single linear polarization. It is no doubt that the polarization diversity can make a harvester more versatile and adaptable [15], [25], [30]. Nevertheless, the diversity is usually at the expense of the size or dimension. The merit of the Yagi antenna, cost effectiveness of the size, could be prominent in circumstances where one linear polarization is obvious or dominant. In light of the fact that linearly polarized antennas are generally equipped in transmitters, some linearly polarized antennas were also frequently adopted for harvesting energy of Digital-TV, FM, communication and Wi-Fi signals [19], [20], [26], [28], [31]–[33].

Printed Yagi and quasi-Yagi antennas evolved into different configurations over these years [17]–[19], [26], [29], [34]–[37]. They usually need relatively large space along the longitudinal direction (the direction of radiating or receiving electromagnetic waves), for holding baluns [28], [34]–[36] or multiple parasitic elements in high-gain designs [17], [26], [28], [29], [36], [37]. It could limit its application scope. In some cases, thin linear antennas like monopoles are preferred in portable devices like WiFi routers, owing to the convenient installation and space saving, especially in a vertical position. Forming an array in the transverse plane can reduce the use of parasitic elements and the longitudinal dimension. However, the array commonly relies on power dividers [19], [35], [36], which still occupy longitudinal space.

In this paper, a quasi-Yagi antenna array driven by a collinear antenna is proposed. The collinear antenna is initially based on the coaxial line (the corresponding design is called coaxial collinear antenna) [38], [39], and then evolves into microstrip versions [40]–[43]. The collinear antenna radiates like a collinear series-fed array of dipoles [44], and hence itself has a function of a power divider. Based on it, the quasi-Yagi antenna array can be easily extended in the collinear direction to obtain a high gain with no extra feeding networks and a reduced number of parasitic elements. Therefore, a high gain can be achieved with a simple, compact and thin profile. Besides, its compactness is further demonstrated by an angle-diversity design that consists of two back-to-back proposed array antennas. The design can compensate the blind spot in the back half space of one array antenna, and nearly double the harvesting coverage with a size less than the sum of two array antennas through sharing reflectors.

In the next section, the driven part, the collinear antenna is analyzed with an equivalent circuit. Then, the effect of parasitic strips and impedance matching are discussed. Based on the analysis, prototypes are designed and fabricated. The measurements of antenna performance and energy harvesting will be provided in Section III.

II. ANTENNA DESIGN

The proposed quasi-Yagi antenna array is depicted in Fig. 1. The driven part, a 4-section collinear antenna, is shown in Fig. 1(a), where the four wide patches with a length of $\lambda_g/2$ (λ_g is the guided wavelength) are etched alternately on the front and back sides, and connected with narrow lines. To enhance the gain of the collinear antenna, a modification is made as illustrated in Fig. 1(b). Each section of the 4-section collinear antenna is with a parasitic strip. Two collinear strips on the right side are shorter than $\lambda_0/2$ (λ_0 is the wavelength in free space) and function as the directors, while two collinear ones on the left side are longer than $\lambda_0/2$ and function as the reflectors. Like other Yagi antennas, the centers of every parasitic strip and driven section are aligned for endfire

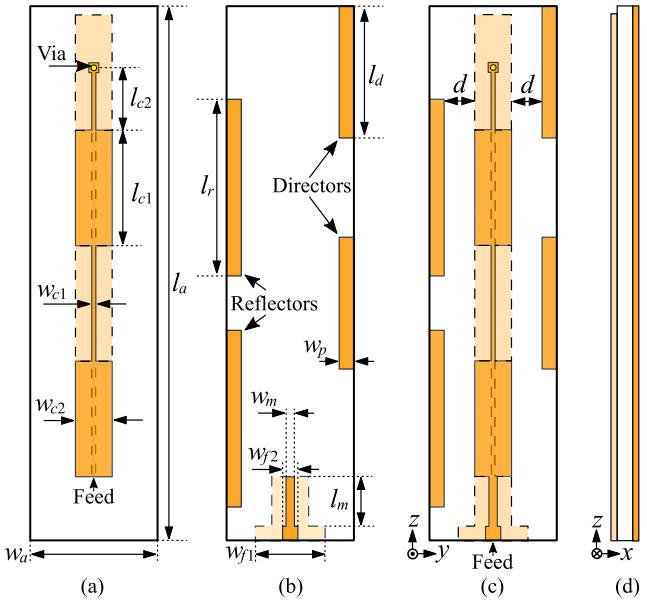

FIGURE 1. Proposed quasi-Yagi antenna array consists of (a) a 4-section collinear antenna with (b) an addition of parasitic strips and a matching circuit. (c) front view, (d) side view. The prototype adopts a 40-mil substrate of Rogers 5880 with $w_a = 26$ mm, $l_a = 190.5$ mm, $w_{c1} = 0.1$ mm, $w_{c2} = 7.5$ mm, $l_{c1} = 41.2$ mm, $l_{c2} = 21.5$ mm, $w_p = 3$ mm, $l_r = 63$ mm, $l_d = 47$ mm, $w_m = 1$ mm, $l_m = 17.8$ mm, $w_{f1} = 15$ mm, $w_{f2} = 3.1$ mm and $d = 6.25$ mm.

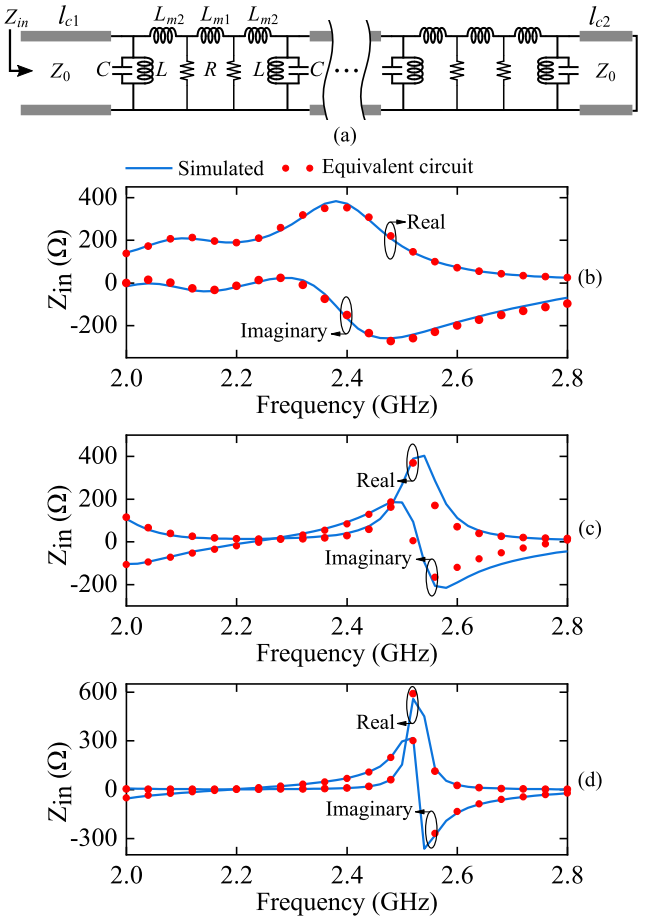

FIGURE 2. Equivalent circuit and input impedance (Z_{in}) of the 4-section collinear antenna in Fig. 1(a). Results in (b), (c) and (d) were respectively obtained with different values of w_{c1}: 0.1, 1.5 and 3.6 mm. In (b), $C = 1.2$ pF, $L = 9.7$ nH, $R = 305$ Ω, $L_{m1} = 9.4$ nH, $L_{m2} = 1.8$ nH; in (c), $C = 0.6$ pF, $R = 780$ Ω, $L_{m1} = 0.05$ nH, $L_{m2} = 2.26$ nH, L is removed; in (d), $C = 0.045$ pF, $R = 5.5$ kΩ, L is removed, L_{m1} and L_{m2} are near zero. These values were obtained by curve fitting.

radiation. The driven part is like a transmission line of two conductors, while the parasitic strips are of single conductor. So the half wavelength of the driven part is more impacted by the substrate, and smaller than that of the parasitic strips. It is the reason why reflectors and directors are both longer than a section of the driven part. Hence, each section resembles a Yagi antenna. In addition, a short line with a width between the narrow lines and the 50-Ω feed line is added for improving impedance matching.

For effectively harvesting wireless energy, the radiation performance is the primary consideration in the design process. The antenna gain is expected to be high in a possibly wider frequency band, while the antenna configuration is supposed to be narrow and compact. In this quasi-Yagi antenna array design, there are two parts affecting the gain performance: the collinear antenna and parasitic strips.

The collinear antenna can be treated as a series-fed array, and thus be able to elevate the gain by merely increasing its elements or sections (length) while maintaining a narrow width. To enhance the radiation in the *xoy* plane, currents on wide patches are supposed to be in phase. Thus the length of every section of the wide patch or narrow line is $\lambda_g/2$. The last narrow line is short-circuited to the wide patch, and its length guarantees current antinodes at midpoints and nodes at edges of sections.

The mechanism of radiating RF waves from collinear sections can be explained by the equivalent circuit in Fig. 2(a). The parasitic capacitor C and inductors L, L_{m2} are induced by the width discontinuity between sections. L is apparent only when the width of narrow lines (w_{c1}) is too small. Power loss including radiation loss, dielectric and conductor loss is reflected by the resistor R. For an antenna with a high radiation efficiency, the radiation loss is the major part. The inductor L_{m1} is caused by the coupling of two adjacent edges of patches, and together with L_{m2}, C and L represents the power transmission or coupling. Since R, C and L are shunt components, and L_{m1} and L_{m2} are series components, a smaller R means more power loss, and a larger L or a smaller C, L_{m1} and L_{m2} indicate more power transmitted or coupled between sections. From Fig. 2(b) to Fig. 2(d), w_{c1} increases from 0.1 to 3.6 mm. With the increase in w_{c1}, R and L become bigger (L is too large and can be ignored in Fig. 2(c) and Fig. 2(d)) while C, L_{m1} and L_{m2} smaller, which means less power radiates per section while more transmits between sections. As a result, power distribution is more uniform on the whole antenna, as demonstrated by the current distributions in Fig. 3(a). Thus, with a larger w_{c1}, more antenna aperture is utilized, and the gain rises. However, when the width of the narrow line w_{c1} further increases, the conductor and dielectric loss could outweigh the radiation, and pull down the radiation

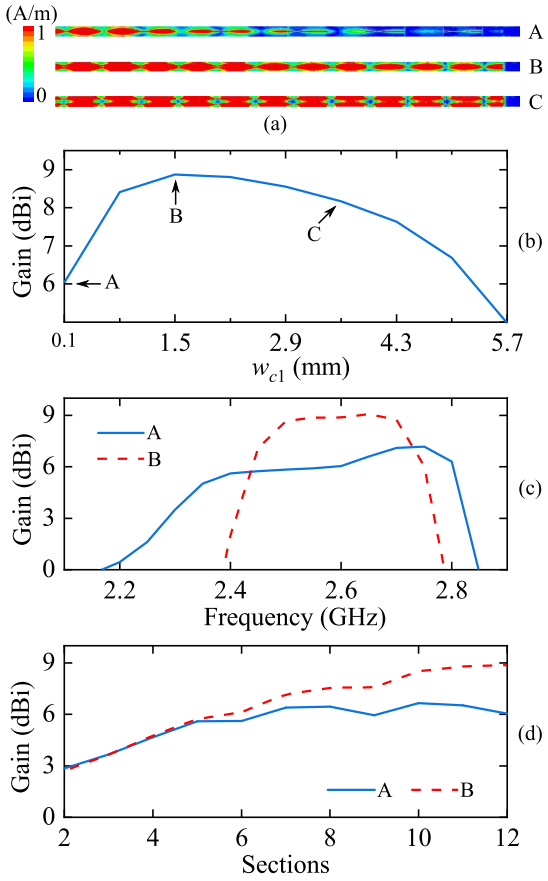

FIGURE 3. Simulated current distribution and *z*-polarized gains at $\varphi = 90°$, $\theta = 90°$. Points A, B and C indicate different values of w_{c1}: 0.1, 1.5 and 3.6 mm. Results in (a), (b) and (d) were obtained at 2.6 GHz, and (a), (b) and (c) were from the simulation of 12-section microstrip collinear antenna.

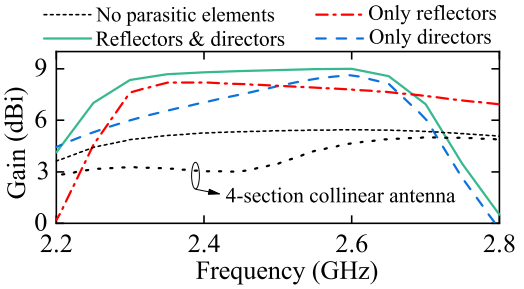

FIGURE 4. *z*-polarized gains of the proposed quasi-Yagi antenna array in Fig. 1 with both of, one of and none of the reflectors and directors.

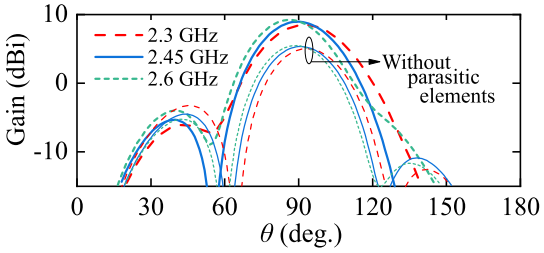

FIGURE 5. Radiation patterns of the proposed quasi-Yagi antenna array at different frequencies.

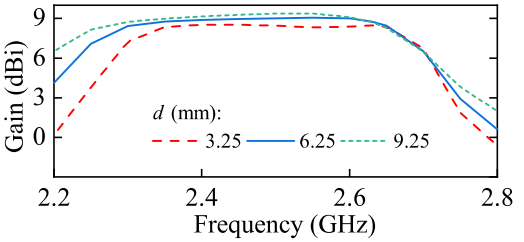

FIGURE 6. *z*-polarized gains of different distances between the parasitic strips and the driven part.

efficiency and the antenna gain. It can be seen in Fig. 3(b) that the gain declines when w_{c1} of the 12-section collinear antenna exceeds 1.5 mm.

Though the gain can reach the peak at $w_{c1} = 1.5$ mm, a smaller value of w_{c1} can strengthen discontinuity and provide a wider bandwidth as illustrated in Fig. 3(c). On the other hand, the width w_{c1} barely affects the gain before the section number reaches 5, as shown in Fig. 3(d). Therefore, the section number and the width of narrow lines w_{c1} are selected to be 4 and 0.1 mm.

The matching circuit connecting the 4-section collinear antenna with the 50-Ω feed line is similar to a section of the collinear antenna. Hence, it also radiates. With the radiation, the gain of the collinear antenna is raised as shown in Fig. 4. The radiation of the matching section, however, is not identical to that of the collinear antenna sections due to a phase difference between their currents. As mentioned above, the sections of the collinear antenna are $\lambda_g/2$ long to assure in-phase currents, while the matching section is shorter than $\lambda_g/2$. As a result of the phase difference, the side lobe of one side is strengthened and the beam becomes obviously asymmetrical as reflected by the radiation patterns in Fig. 5. Considering that the excitation phase of the elements of a series-fed antenna array is usually frequency dependent and the beam angle could scan with frequency, beam patterns at different frequencies are also provided. It can be found that, due to the driven part the collinear antenna, the beam angle of the quasi-Yagi antenna array varies in a small range from 92° to 86° when the frequency increases from 2.3 to 2.6 GHz (it is 90° at 2.45 GHz). The endfire radiation pattern is relatively stable in the frequency band.

Each section of the collinear antenna is a driven element, and the centers of each driven element and its corresponding parasitic element are aligned for endfire radiation. Since parasitic strips are longer than the collinear section, they are alternately etched on the left and right sides, and respectively function as reflective and directive elements. As illuminated in Fig. 4, though with only two reflectors or directors for four sections, the gain can already noticeably increase from around 5 dBi to more than 8 dBi in a lower or upper frequency band. With both of them, the gain can reach around 9 dBi in a wide band. The distance between the parasitic strips and the driven part (denoted as *d* in Fig. 1) is an important factor affecting the gain. As shown in Fig. 6, a larger distance results

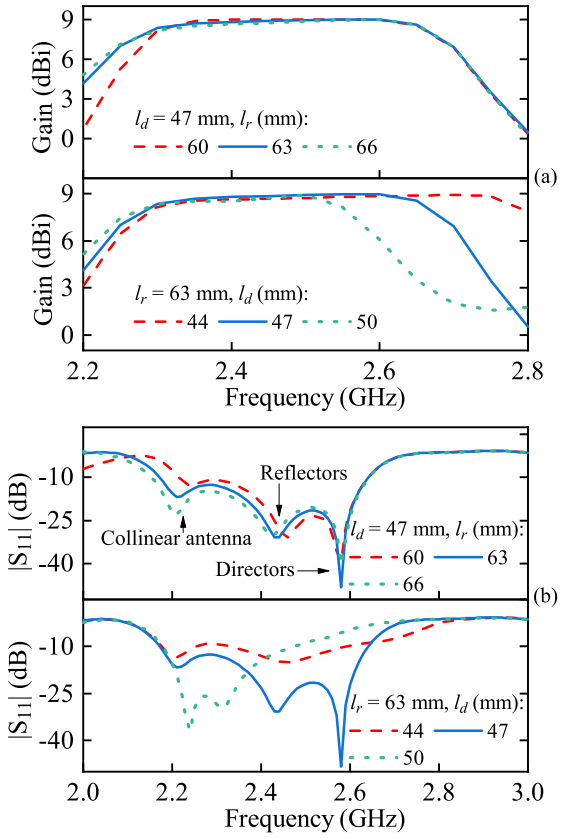

FIGURE 7. (a) *z*-polarized gains and (b) reflection coefficients of different lengths of reflectors and directors.

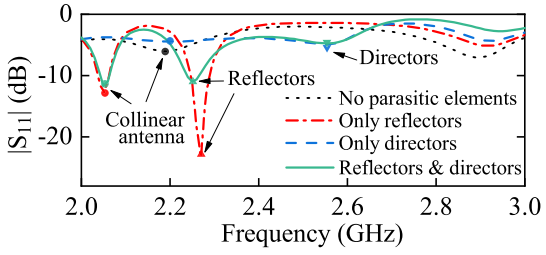

FIGURE 8. Reflection coefficients of the quasi-Yagi antenna array without the matching circuit.

in a higher gain and a larger bandwidth. After balancing the performance and the width (or size), d is 6.25 mm in the proposed design. The lengths of the reflectors and directors also impact the gain bandwidth. From the results in Fig. 7, the quasi-Yagi antenna array is more sensitive to the length of directors rather than reflectors. This phenomenon is also found in the impedance matching. The extra matching poles introduced by reflectors and directors shift more dramatically when the length of directors is varied. By properly adjusting the lengths of directors and reflectors, different operating frequency bands can be obtained.

Nevertheless, by comparing the reflection coefficients in Fig. 7 and Fig. 8, it can be found that the impedance matching is still not acceptable with only matching poles introduced by parasitic strips, though it is improved. In Fig. 7,

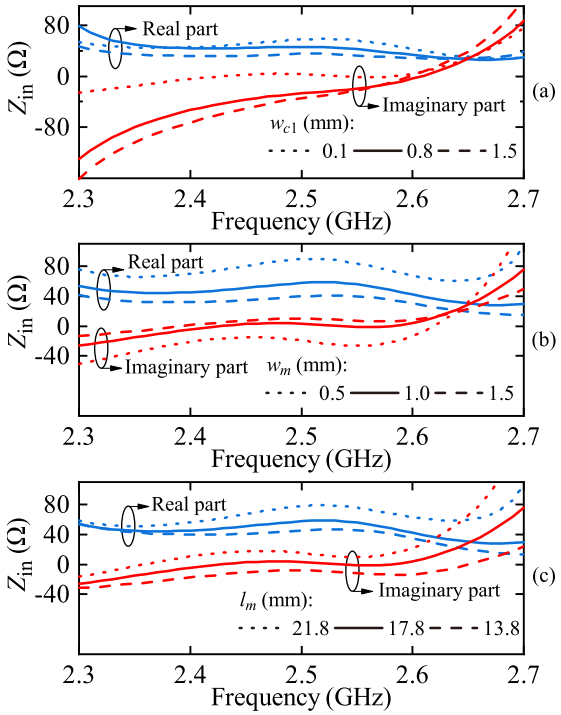

FIGURE 9. Input impedances of different (a) widths of narrow connecting lines, (b) widths and (c) lengths of the short matching line.

a simple matching circuit, a short line, is also employed. It can effectively adjust both the real and imaginary parts of the input impedance as illustrated in Fig. 9, and fulfill impedance matching of narrower or wider frequency bands. As mentioned above, the width of narrow connecting lines (w_{c1}) regulates the radiated power of each section, and from another perspective, it changes the Q factor or the impedance bandwidth. It can be verified by the first graph of Fig. 9, where a wider narrow line induces a steeper slope of the imaginary part. The width and length of the additional short line are both useful in altering the input impedance. A larger width or a smaller length can reduce the real part, while a larger width or length can elevate the imaginary part. According to the trend reflected by Fig. 9, impedance matching can be implemented in the following way. If a wider bandwidth is needed, narrow lines could be thinner. The real and imaginary parts will be then elevated. To adapt the change and cancel the impedance increase, the matching line could be appropriately wider and shorter.

III. MEASURED PERFORMANCE

Wide angle coverage can improve the capability of exploiting ambient energy coming from different directions. An angle-diversity prototype is hence presented to demonstrate the compactness. It is simply composed of two back-to-back quasi-Yagi antenna arrays and has two ports that separately offer two independent beams. Through sharing one set of reflectors, it is smaller than the size of two antenna arrays, as shown by the photograph in Fig. 10. It is denoted

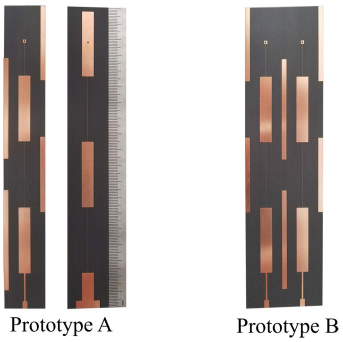

FIGURE 10. Fabricated quasi-Yagi antenna array (prototype A) and its derived angle-diversity design (prototype B). Prototype B consists of two back-to-back quasi-Yagi arrays, and its width is 49 mm, smaller than the sum of widths of two array antennas.

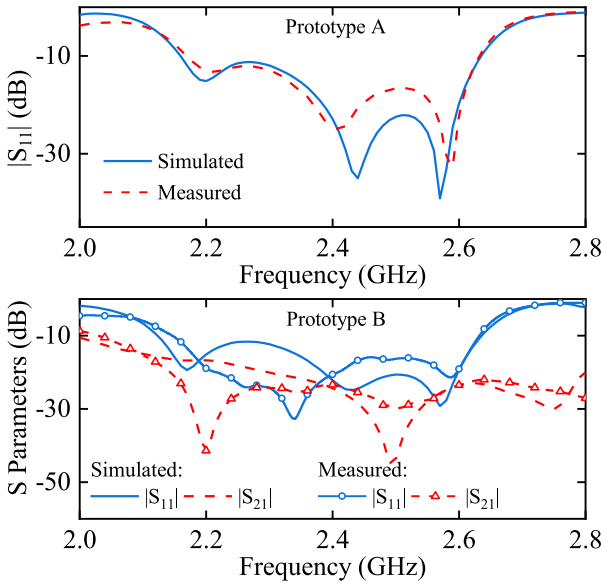

FIGURE 11. S parameters of the proposed prototypes A and B.

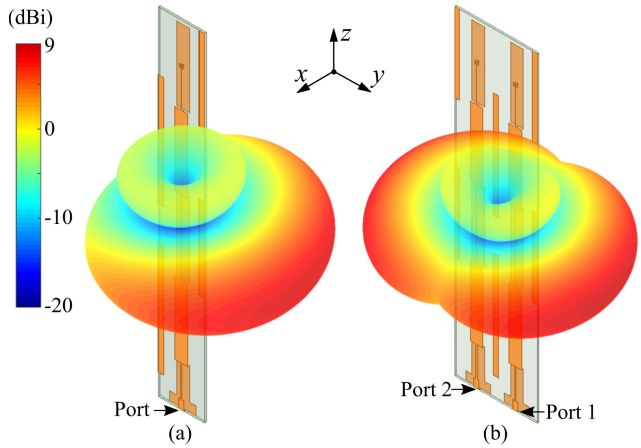

FIGURE 12. Radiation patterns of (a) the quasi-Yagi antenna array (prototype A) and (b) the derived angle-diversity design (prototype B). In (b), two beams excited respectively by port 1 and port 2 are overlapped to illustrate the expansion of coverage.

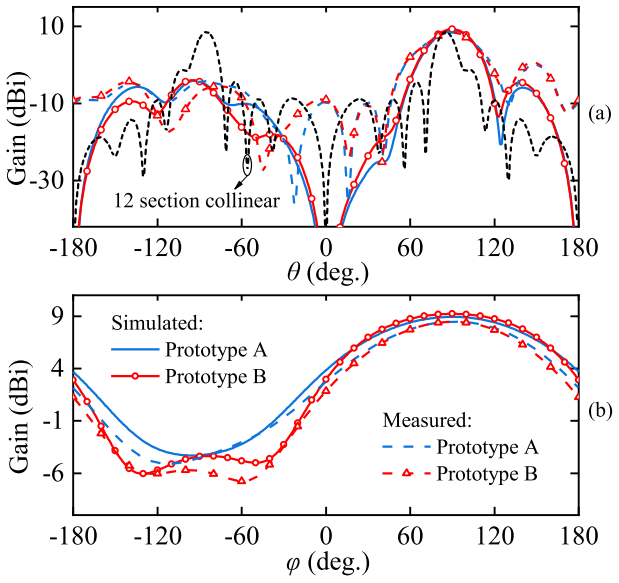

FIGURE 13. (a) E-plane (*yoz*) and (b) H-plane (*xoy*) θ-polarized patterns of prototypes A and B at 2.45 GHz. The E-plane pattern of the 12-section collinear antenna with $w_{c1} = 1.5$mm is also presented for comparison.

as prototype B, while the single quasi-Yagi antenna array denoted as prototype A.

A. ANTENNA PERFORMANCE

In the frequency band from 2.18 to 2.63 GHz, these two proposed prototypes are both well matched according to the simulated and measured S parameters in Fig. 11. Though two arrays of prototype B simply duplicate the configuration of prototype A and even share reflectors, the isolation between two ports of prototype B is better than 20 dB in a wide band. The results from the simulation and measurement are generally consistent. The difference in the curves of prototype B is bigger since the curving or warping caused by the fabrication is more obvious on the larger flexible substrate.

The two prototypes of quasi-Yagi antenna arrays are linearly polarized (*z*-polarized), and their overall radiation patterns, namely the spatial coverages, are illustrated in Fig. 12. The E-plane and H-plane patterns are depicted in Fig. 13. It shows that the collinear antenna itself needs 12 sections and a large length to reach a gain close to the proposed designs. The solution, loading parasitic strips, can reduce the demand for sections, then shorten the length and widen the E-plane beamwidth, thus make the antenna design more practical. Patterns of two prototypes are almost same, and the E- and H-plane 3-dB beamwidths can be more than 30° and 123° respectively. From 2.3 to 2.63 GHz, the forward gains of A and B respectively are 8.04–8.73 dBi and 8.24–8.62 dBi from the measured results, and are 8.46–9.04 dBi and 8.90–9.24 dBi from the simulated results, as shown in Fig. 14. The in-band decrease of measured gains is probably due to a few fabrication flaws on the 0.1-mm narrow lines and the warping of the flexible substrate, while the out-of-band decrease due to the return loss included in measured results. From these results of radiation performance, these two

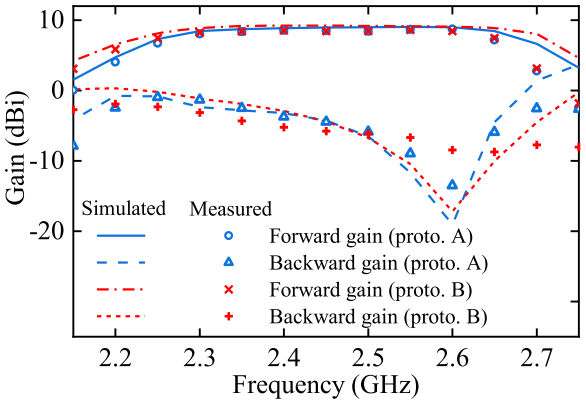

FIGURE 14. *z*-polarized gains of the two prototypes. Results of prototype B were attained under the condition that one port was excited and the other one was connected to a 50-Ω load.

prototypes are with relatively small back lobes. The back lobe can approach −20 dBi at 2.6 GHz, and rises in the lower and upper segments of the frequency band. It is because that the reflective and directive loading of parasitic strips is frequency dependent. To pursue a compact configuration, the frequency of the lowest back lobe is designed to be higher than the operating frequency. According to the literature [40], [42], [43] and the pattern of the 12-section collinear antenna in Fig. 13(a), the level of side lobes of the microstrip collinear antenna is usually around −10 dBi. Due to the phase difference between radiation of the matching circuit and the 4-section collinear antenna, the side lobe of one side is strengthened. However, the level of side lobes is still relatively low.

To measure the compactness of the proposed quasi-Yagi antenna array, the ratio of the effective antenna aperture to the physical size A_e/A_p is utilized ($A_e=G\times\lambda_0^2/4\pi$, G is the antenna gain). From the comparison of antennas for wireless energy harvesting in Table 1, it can be concluded that, except the electrically small antenna like [5], which presents a very compact size at the cost of low gains, Yagi antennas can provide high gains with the most compact size. Compared to other Yagi antennas, the proposed quasi-Yagi array design owns a comparably compact size and maintains a stable high gain in a wide band. Its narrowest configuration means the lowest demand for space along the direction of incident RF waves, which would make it more suitable for portable harvesters with confined space. If a thinner size is expected, the proposed design can reduce the width of patches and the distance between parasitic strips and the collinear antenna at the cost of a narrower frequency bandwidth.

B. PERFORMANCE OF ENERGY HARVESTING

To demonstrate the performance of energy harvesting, a rectifying circuit shown in Fig. 15 is adopted. The circuit is designed with a Schottky diode SMS7630 at 2.45 GHz and fabricated on a 20-mil substrate of Rogers 5880. The measured results in Fig. 16 show that the efficiency of a single rectifying circuit is more than 40% from 2.41 to 2.49 GHz,

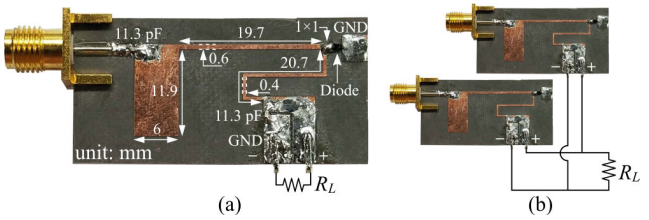

FIGURE 15. Rectifying circuits used in the harvesting measurements: (a) a single rectifying circuit for prototype A, (b) two such circuits with their dc pins connected in parallel for prototype B. A 2.5-kΩ resistor R_L served as the dc load of these two prototypes. The voltage across the dc load is denoted as V_{dc}. The rectified dc power is $P_{dc} = V_{dc}^2/R_L$.

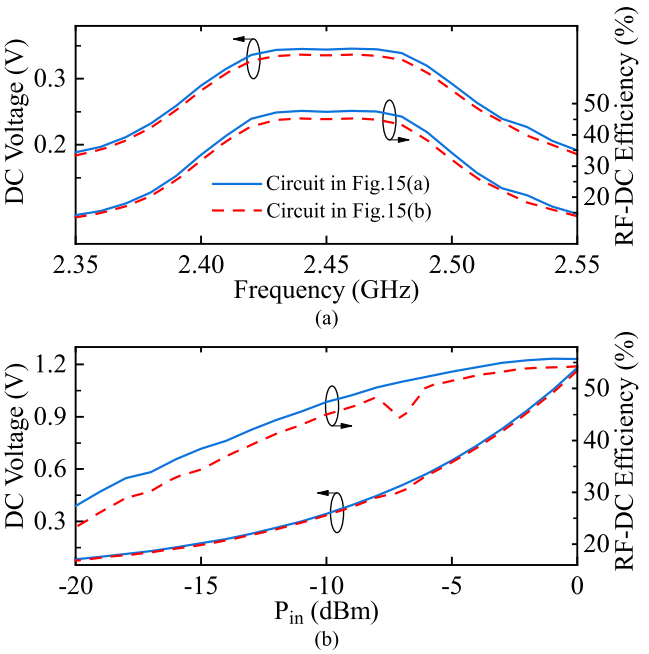

FIGURE 16. Rectified dc voltage and RF-dc conversion efficiency of rectifying circuits for prototypes A and B varying with (a) frequency and (b) input RF power. The circuits were measured with input RF power of −10 dBm in (a), and measured at 2.45 GHz in (b). When measuring the circuit in Fig. 15(b), only one port was fed with RF power.

and obtains a peak value of 47.7% at −10-dBm RF power. With the RF power ranging from −20 to 0 dBm, the efficiency varies from 27.4% to 55.7%. Since two beams provided respectively by the two ports of prototype B are back to back, the major harvesting coverage areas of two beams are not overlapped. Furthermore, two ports are isolated well. Every beam can thus be treated as independent. Therefore, two rectifying circuits in Fig. 15(a) are directly used to convert the RF power from two ports of prototype B. Their dc pins are connected in parallel, namely in a form of current summing, as shown in Fig. 15(b). The angle-diversity harvester probably absorbs energy from only one direction. Under this circumstance, one rectifying branch is activated and the other one, especially its diode, simply consumes power. To examine the power loss, the rectifier in Fig. 15(b) was measured with only one port fed with RF power. The corresponding results in Fig. 16 indicate that the efficiency loss is generally low, and slightly higher in the low power region.

TABLE 1. Comparison of the proposed rectennas with previous designs for wireless energy harvesting.

Reference	Ant. Freq. (GHz)	Beams	Dimension (mm^3)	Gain (dBi)	A_e/A_p	η_{RF-dc} (%)
Koch fractal loop [5]	1.76–1.87	1	45×45×0.8	3	2.18 @1.8 GHz	~42.8 @1 μW/cm^2
Cross-dipole [30]	1.8–2.5	1	70×70×13.2	3.5 @2.15 GHz	0.71 @2.15 GHz	~47 @1 μW/cm^2, 2.15 GHz
6-element Yagi [17]	2.45	1	57.5×159×NA	11.8	1.97	~53.4 @1 μW/cm^2
3-element Yagi [18]	0.915, 2.45	1	56.46×61.5×0.0254	7.59 @2.45 GHz	1.97 @2.45GHz	~51.3 @1 μW/cm^2, 2.45 GHz
Yagi array [19]	1.78–2.22	1	100×190×1.6	7.8–11.6	0.7–1.18	~30.5–55 @0.05–1 μW/cm^2, 2.14 GHz
Suspended patches [21]	2.43-2.52	1	60×100×7	5.9	0.77 @2.45 GHz	~25 @1 μW/cm^2 with PMN
		2	120×100×7	8.7	0.74 @2.45 GHz	~41 @1 μW/cm^2 with PMN
		4	240×100×7	9.7	0.46 @2.45 GHz	~44 @1 μW/cm^2 with PMN
Grid array [23]	2.45	2	226×337×16	15.5	0.56	16.3–45.3 @0.052–1 μW/cm^2
5 patch arrays [22]	2.4-2.43	20	290×130^2×π (290×81.7×0.72)	8.84	0.40 @2.4 GHz	45 @1 μW/cm^2
4 Yagi antennas [26]	2.24-2.48	4	60×60×60 (60×60×0.175)	5.96	1.31 @2.45 GHz	6.4 @0.01 μW/cm^2
2 suspended patches [25]	0.9–0.96, 1.8–2.18	2	175×200×49.6 (175×200×24.7)	8.15 @2.15GHz	0.29 @2.15GHz	40 @0.05 μW/cm^2 (with 3 tones: 0.925, 1.85 & 2.15 GHz)
Prototype A† (This work)	2.3–2.63	1	26×190.5×1.5	8.04–8.73 (8.46–9.04)	1.41–1.81 (1.57–1.96)	23.8–46.7 @0.05–1 μW/cm^2, 2.45 GHz
Prototype B† (This work)	2.3–2.63	2	49×190.5×1.5 (24.5×190.5×1.5)	8.24–8.62 (8.90–9.24)	1.47–1.95 (1.76–2.29)	23.7–47.0 @0.05–1 μW/cm^2, 2.45 GHz

*Beams are back to back in this work and [25], while are adjacent in [21]–[23], [26]. The dimension values in brackets are the volume of one element antenna or one array of the multi-directional rectenna, and used in the calculation of A_e/A_p. The heights or thicknesses of antennas are not included in A_p. The RF-to-dc conversion efficiency in [21] is measured with a power management network (PMN).

†The simulated results of the proposed designs are given in brackets. And their frequency values indicate the high-gain bandwidths, and the measured impedance bandwidth is from 2.18 to 2.63 GHz.

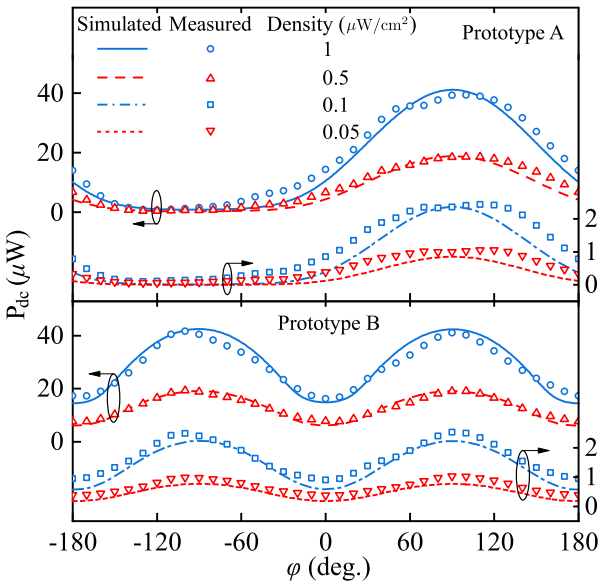

FIGURE 17. Energy harvesting patterns of rectennas based on the two prototypes. In the measurement, the RF power density ranged from 0.05 to 1 μW/cm^2.

The harvesting patterns of two prototypes are presented in Fig. 17. For prototype A, the dc power at the angle of forward radiation of antennas reached 1, 2.4, 18.4 and 39.2 μW under power densities of 0.05, 0.1, 0.5 and 1 μW/cm^2, and for prototype B it reached 1, 2.5, 19 and 41 μW. The RF-to-dc conversion efficiency can be expressed as η_{RF-dc}=P$_{dc}$/(A_e×D), where D is the power density. If measured gains are used in the calculation, the corresponding efficiencies are 23.8%, 28.3%, 43.9% and 46.7% for prototype A, and 23.7%, 28.9%, 43.5% and 47.0% for prototype B. If simulated gains are used, they are 21.5%, 25.5%, 39.5% and 42.0% for prototype A, and 19.9%, 24.3%, 36.6% and 39.5% for prototype B. In an azimuth angle range of 100°, prototype A can produce dc power of more than 0.8, 1.9, 14 and 31 μW at 0.05, 0.1, 0.5 and 1 μW/cm^2. The coverage of prototype B is nearly doubled, where the dc output is more than 0.6, 1.5, 12 and 27 μW respectively for these four power densities.

The state-of-the-art performance of rectennas for wireless energy harvesting is listed in Table 1. Rectennas of low gains can perform well at lower frequencies since the effective antenna aperture and the RF-to-dc conversion efficiency are larger and higher. With the frequency increasing, the gain should be higher to make the rectifying circuit operate in its high-efficiency zone. Thanks to the high gain, the rectification efficiency of the proposed rectennas maintains relatively high levels at low power densities. The proposed rectennas were measured at a single frequency. A higher efficiency can be obtained with multifrequency RF waves illuminating the rectenna. Compared with other rectennas with two beams for wider coverage in Table 1, this work (prototype B) presents the most compact configuration, owing to the benefit of high space utilization of the quasi-Yagi antenna array (prototype A). Therefore, it can be deduced that two sets of antennas like prototype B perpendicular to each other (one is in *yoz*, the other in *xoz* plane and all their reflectors are collinear) can make the harvesting coverage omnidirectional in the horizontal plane with a still compact configuration.

The rectenna designs were also measured with WiFi signals as demonstrated in Fig. 18. The output of the dc voltage rippled as shown in Fig. 19. To evaluate their performance, root-mean-square (RMS) values of the dc voltages of the whole measured period in Fig. 19 were calculated. When d_1 = 1 m and d_2 = 1.5 m, the RMS voltages of prototypes A and B are 0.863 and 0.879 V. When d_1 = 1.5 m, d_2 = 1 m,

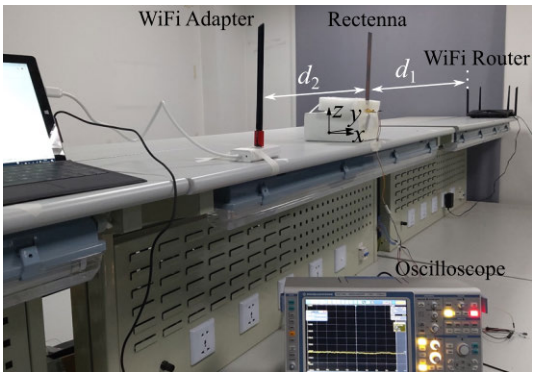

FIGURE 18. Setup for measurement of WiFi energy harvesting. The rectennas based on prototypes A and B respectively stood between the WiFi router and the USB WiFi adapter. The distances are denoted as d_1 and d_2. In the measurement, the laptop was continuously downloading files. A capacitor of 100 μF was added in parallel with the 2.5-kΩ resistor to smooth the output. In this picture, $d_1 = 2$ m and $d_2 = 0.5$ m.

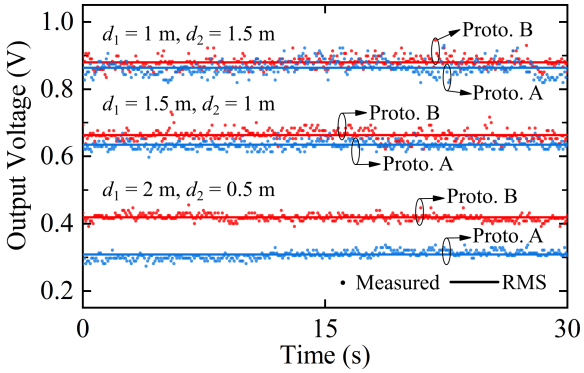

FIGURE 19. Output voltages measured at different locations between the WiFi router and the adapter.

they are 0.635 and 0.664 V. When $d_1 = 2$ m, $d_2 = 0.5$ m, they are 0.308 and 0.418 V. Since the power emitted from the router is much higher than that of the adapter, the output decreased with the distance d_1. According to the RMS voltages, the prototype B performed better due to the improved and doubled spatial coverage.

IV. CONCLUSION

A novel compact thin configuration is proposed for a quasi-Yagi antenna array. The collinear antenna as the driven part resembles a series-fed array of dipoles. It can easily increase the gain by extending the transverse dimension without extra power dividers, reduce the use of parasitic elements, and thus permits a narrow width. Only one piece of a short strip line is adopted to realize impedance matching in a frequency band over 300 MHz. A rectenna based on it could stably harvest RF energy due to the steady and high gains in the operating frequency range. The narrowed width can make the quasi-Yagi antenna array more space-saving and fit for portable harvesters as well as communication devices.

REFERENCES

[1] S. Ladan, N. Ghassemi, A. Ghiotto, and K. Wu, "Highly efficient compact rectenna for wireless energy harvesting application," *IEEE Microw. Mag.*, vol. 14, no. 1, pp. 117–122, Jan. 2013.

[2] K. Niotaki, S. Kim, S. Jeong, A. Collado, A. Georgiadis, and M. M. Tentzeris, "A compact dual-band rectenna using slot-loaded dual band folded dipole antenna," *IEEE Antennas Wireless Propag. Lett.*, vol. 12, pp. 1634–1637, 2013.

[3] J. Wu Zhang, K. Yak See, and T. Svimonishvili, "Printed decoupled dual-antenna array AC for small wirelessly powered battery-less device," *IEEE Antennas Wireless Propag. Lett.*, vol. 13, pp. 923–926, 2014.

[4] Y.-S. Chen and C.-W. Chiu, "Maximum achievable power conversion efficiency obtained through an optimized rectenna structure for RF energy harvesting," *IEEE Trans. Antennas Propag.*, vol. 65, no. 5, pp. 2305–2317, May 2017.

[5] M. Zeng, A. S. Andrenko, X. Liu, Z. Li, and H.-Z. Tan, "A compact fractal loop rectenna for RF energy harvesting," *IEEE Antennas Wireless Propag. Lett.*, vol. 16, pp. 2424–2427, 2017.

[6] W. Lin, R. W. Ziolkowski, and J. Huang, "Electrically small, low-profile, highly efficient, Huygens dipole rectennas for wirelessly powering Internet-Things devices," *IEEE Trans. Antennas Propag.*, vol. 67, no. 6, pp. 3670–3679, Jun. 2019.

[7] M. K. Hosain, A. Z. Kouzani, M. F. Samad, and S. J. Tye, "A miniature energy harvesting rectenna for operating a head-mountable deep brain stimulation device," *IEEE Access*, vol. 3, pp. 223–234, 2015.

[8] U. Olgun, J. L. Volakis, and C.-C. Chen, "Design of an efficient ambient WiFi energy harvesting system," *IET Microwaves, Antennas Propag.*, vol. 6, no. 11, pp. 1200–1206, Aug. 2012.

[9] U. Olgun, C.-C. Chen, and J. L. Volakis, "Investigation of rectenna array configurations for enhanced RF power harvesting," *IEEE Antennas Wireless Propag. Lett.*, vol. 10, pp. 262–265, 2011.

[10] S. D. Assimonis, S.-N. Daskalakis, and A. Bletsas, "Sensitive and efficient RF harvesting supply for batteryless backscatter sensor networks," *IEEE Trans. Microw. Theory Techn.*, vol. 64, no. 4, pp. 1327–1338, Apr. 2016.

[11] S. Hemour, Y. Zhao, C. H. P. Lorenz, D. Houssameddine, Y. Gui, C.-M. Hu, and K. Wu, "Towards low-power high-efficiency RF and microwave energy harvesting," *IEEE Trans. Microw. Theory Techn.*, vol. 62, no. 4, pp. 965–976, Apr. 2014.

[12] C. H. P. Lorenz, S. Hemour, W. Li, Y. Xie, J. Gauthier, P. Fay, and K. Wu, "Breaking the efficiency barrier for ambient microwave power harvesting with heterojunction backward tunnel diodes," *IEEE Trans. Microw. Theory Techn.*, vol. 63, no. 12, pp. 4544–4555, Dec. 2015.

[13] H. Sun and W. Geyi, "A new rectenna using beamwidth-enhanced antenna array for RF power harvesting applications," *IEEE Antennas Wireless Propag. Lett.*, vol. 16, pp. 1451–1454, 2017.

[14] Y. Ushijima, T. Sakamoto, E. Nishiyama, M. Aikawa, and I. Toyoda, "5.8-GHz integrated differential rectenna unit using both-sided MIC technology with design flexibility," *IEEE Trans. Antennas Propag.*, vol. 61, no. 6, pp. 3357–3360, Jun. 2013.

[15] C. Song, Y. Huang, P. Carter, J. Zhou, S. D. Joseph, and G. Li, "Novel compact and broadband frequency-selectable rectennas for a wide input-power and load impedance range," *IEEE Trans. Antennas Propag.*, vol. 66, no. 7, pp. 3306–3316, Jul. 2018.

[16] H. Sun, Y. Guo, M. He, and Z. Zhong, "Design of a high-efficiency 2.45-GHz rectenna for low-input-power energy harvesting," *IEEE Antennas Wireless Propag. Lett.*, vol. 11, pp. 929–932, 2012.

[17] P. Soboll, V. Wienstroer, and R. Kronberger, "Smooth moves in power transition: New Yagi–Uda antenna design for wireless energy," *IEEE Microw. Mag.*, vol. 17, no. 5, pp. 75–80, May 2016.

[18] R. Scheeler, S. Korhummel, and Z. Popovic, "A dual-frequency ultralow-power efficient 0.5-g rectenna," *IEEE Microw. Mag.*, vol. 15, no. 1, pp. 109–114, Jan. 2014.

[19] H. Sun, Y.-X. Guo, M. He, and Z. Zhong, "A dual-band rectenna using broadband Yagi antenna array for ambient RF power harvesting," *IEEE Antennas Wireless Propag. Lett.*, vol. 12, pp. 918–921, 2013.

[20] Y.-S. Chen, F.-P. Lai, and J.-W. You, "Analysis of antenna radiation characteristics using a hybrid ray tracing algorithm for indoor WiFi energy-harvesting rectennas," *IEEE Access*, vol. 7, pp. 38833–38846, 2019.

[21] D.-J. Lee, S.-J. Lee, I.-J. Hwang, W.-S. Lee, and J.-W. Yu, "Hybrid power combining rectenna array for wide incident angle coverage in RF energy transfer," *IEEE Trans. Microw. Theory Techn.*, vol. 65, no. 9, pp. 3409–3418, Sep. 2017.

[22] E. Vandelle, D. H. N. Bui, T.-P. Vuong, G. Ardila, K. Wu, and S. Hemour, "Harvesting ambient RF energy efficiently with optimal angular coverage," *IEEE Trans. Antennas Propag.*, vol. 67, no. 3, pp. 1862–1873, Mar. 2019.

[23] Y.-Y. Hu, S. Sun, H. Xu, and H. Sun, "Grid-array rectenna with wide angle coverage for effectively harvesting RF energy of low power density," *IEEE Trans. Microw. Theory Techn.*, vol. 67, no. 1, pp. 402–413, Jan. 2019.

[24] Y.-Y. Hu and S. Sun, "Dual-polarized and multi-beam cross-mesh array antenna for RF energy harvesting applications," in *Proc. IEEE Int. Symp. Antennas Propag. USNC/URSI Nat. Radio Sci. Meeting*, Jul. 2018, pp. 2527–2528.

[25] S. Shen, C.-Y. Chiu, and R. D. Murch, "A dual-port triple-band L-probe microstrip patch rectenna for ambient RF energy harvesting," *IEEE Antennas Wireless Propag. Lett.*, vol. 16, pp. 3071–3074, 2017.

[26] D. H. N. Bui, T.-P. Vuong, J. Verdier, B. Allard, and P. Benech, "Design and measurement of 3D flexible antenna diversity for ambient RF energy scavenging in indoor scenarios," *IEEE Access*, vol. 7, pp. 17033–17044, 2019.

[27] J. Kimionis, M. Isakov, B. S. Koh, A. Georgiadis, and M. M. Tentzeris, "3D-printed origami packaging with inkjet-printed antennas for RF harvesting sensors," *IEEE Trans. Microw. Theory Techn.*, vol. 63, no. 12, pp. 4521–4532, Dec. 2015.

[28] Y.-S. Chen and J.-W. You, "A scalable and multidirectional rectenna system for RF energy harvesting," *IEEE Trans. Compon., Packag., Manuf. Technol.*, vol. 8, no. 12, pp. 2060–2072, Dec. 2018.

[29] F. Fezai, C. Menudier, M. Thevenot, T. Monediere, and N. Chevalier, "Multidirectional receiving system for RF to dc conversion signal: Application to home automation devices," *IEEE Antennas Propag. Mag.*, vol. 58, no. 3, pp. 22–30, Jun. 2016.

[30] C. Song, Y. Huang, J. Zhou, J. Zhang, S. Yuan, and P. Carter, "A high-efficiency broadband rectenna for ambient wireless energy harvesting," *IEEE Trans. Antennas Propag.*, vol. 63, no. 8, pp. 3486–3495, Aug. 2015.

[31] R. J. Vyas, B. B. Cook, Y. Kawahara, and M. M. Tentzeris, "E-WEHP: A batteryless embedded sensor-platform wirelessly powered from ambient digital-TV signals," *IEEE Trans. Microw. Theory Techn.*, vol. 61, no. 6, pp. 2491–2505, Jun. 2013.

[32] M. Pinuela, P. D. Mitcheson, and S. Lucyszyn, "Ambient RF energy harvesting in urban and semi-urban environments," *IEEE Trans. Microw. Theory Techn.*, vol. 61, no. 7, pp. 2715–2726, Jul. 2013.

[33] S. N. Daskalakis, J. Kimionis, A. Collado, G. Goussetis, M. M. Tentzeris, and A. Georgiadis, "Ambient backscatterers using FM broadcasting for low cost and low power wireless applications," *IEEE Trans. Microw. Theory Techn.*, vol. 65, no. 12, pp. 5251–5262, Dec. 2017.

[34] I.-J. Hwang, B. Ahn, S.-C. Chae, J.-W. Yu, and W.-W. Lee, "Quasi-Yagi antenna array with modified folded dipole driver for mmWave 5G cellular devices," *IEEE Antennas Wireless Propag. Lett.*, vol. 18, no. 5, pp. 971–975, May 2019.

[35] W. R. Deal, N. Kaneda, J. Sor, Y. Qian, and T. Itoh, "A new quasi-Yagi antenna for planar active antenna arrays," *IEEE Trans. Microw. Theory Techn.*, vol. 48, no. 6, pp. 910–918, Jun. 2000.

[36] F. Sun, F.-S. Zhang, H. Zhang, H. Zhang, C. Li, and C. Feng, "A frequency diversity printed-Yagi antenna element for apertures selectivity wideband array application," *IEEE Trans. Antennas Propag.*, vol. 66, no. 10, pp. 5634–5638, Oct. 2018.

[37] G. R. DeJean, T. T. Thai, S. Nikolaou, and M. M. Tentzeris, "Design and analysis of microstrip bi-Yagi and quad-Yagi antenna arrays for WLAN applications," *IEEE Antennas Wireless Propag. Lett.*, vol. 6, pp. 244–248, 2007.

[38] H. Wheeler, "A vertical antenna made of transposed sections of coaxial cable," in *Proc. IRE Int. Conv. Rec.*, vol. 4, Mar. 2005, pp. 160–164.

[39] B. Balsley and W. Ecklund, "A portable coaxial collinear antenna," *IEEE Trans. Antennas Propag.*, vol. AP-20, no. 4, pp. 513–516, Jul. 1972.

[40] R. Bancroft and B. Bateman, "An omnidirectional planar microstrip antenna," *IEEE Trans. Antennas Propag.*, vol. 52, no. 11, pp. 3151–3153, Nov. 2004.

[41] R. M. Rudish, "Comments on 'an omnidirectional planar microstrip antenna,'" *IEEE Trans. Antennas Propag.*, vol. 53, no. 11, p. 3855, Nov. 2005.

[42] L. Wang, K. Wei, J. Feng, Z. Zhang, and Z. Feng, "A wideband omnidirectional planar microstrip antenna for WLaN applications," in *Proc. IEEE Elect. Design Adv. Packag. Syst. Symp. (EDAPS)*, Dec. 2011, pp. 1–4.

[43] J. Tang, L. Fang, and H. Cheng, "A low sidelobe and high gain omnidirectional COCO antenna array," in *Proc. 3rd Asia–Pacific Conf. Antennas Propag.*, Jul. 2014, pp. 339–341.

[44] X. Qing and Z. N. Chen, "Omnidirectional antennas," in *Handbook of Antenna Technologies*. Singapore: Springer, 2015, pp. 1–53.

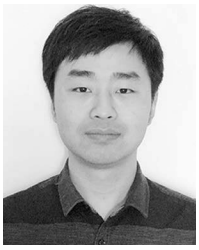

YI-YAO HU (Student Member, IEEE) received the B.Eng. degree in electronic engineering from the University of Electronic Science and Technology of China, Chengdu, China, in 2013, where he is currently pursuing the Ph.D. degree.

His current research interests include wireless power transfer and harvesting, rectifying antennas, and power management circuits.

Mr. Hu was a recipient of the Third and Second place awards of the Student Design Competition (Wireless Energy Harvesting) of the IEEE International Microwave Symposium, in 2014 and 2015, respectively.

SHENG SUN (Senior Member, IEEE) received the B.Eng. degree in information engineering from Xi'an Jiaotong University, Xi'an, China, in 2001, and the Ph.D. degree in electrical and electronic engineering from Nanyang Technological University (NTU), Singapore, in 2006.

From 2005 to 2006, he was with the Institute of Microelectronics, Singapore. From 2006 to 2008, he was a Postdoctoral Research Fellow at NTU. From 2008 to 2010, he was a Humboldt Research Fellow at the Institute of Microwave Techniques, University of Ulm, Ulm, Germany. From 2010 to 2015, he was a Research Assistant Professor with The University of Hong Kong, Hong Kong. Since 2015, he has been a Full Professor with the University of Electronic Science and Technology of China, Chengdu, China. He has authored or coauthored one book and two book chapters, and over 170 journal and conference publications. His current research interests include electromagnetic theory, computational electromagnetics, multiphysics, numerical modeling of planar circuits and antennas, microwave passive and active devices, and the microwave- and millimeter-wave communication systems.

Prof. Sun was a recipient of the ISAP Young Scientist Travel Grant, Japan, in 2004, the Hildegard Maier Research Fellowship of the Alexander Von Humboldt Foundation, Germany, in 2008, the Outstanding Reviewer Award of the IEEE Microwave and Wireless Components Letters, in 2010, as well as the General Assembly Young Scientists Award from the International Union of Radio Science, in 2014. He is currently a member of the Editor Board of the *International Journal of RF and Microwave Computer Aided Engineering*, and serves as an Associate Editor for the IEEE Microwave and Wireless Components Letters and the *IET Electronics Letters*. From 2010 to 2014, he was as an Associate Editor of the *IEICE Transactions on Electronics*, and has served as a Guest Associate Editor for the *Applied Computational Electromagnetics Society Journal*, in 2017, and the IEEE Journal on Multiscale and Multiphysics Computational Techniques, in 2018.

HAO XU was born in Shenyang, China. He received the B.S. degree in electromagnetic field and radio technology, and the M.E. degree in electronics and communication engineering from the University of Electronic Science and Technology of China, Chengdu, China, in 2015 and 2018, respectively.

His current research interest includes differentially-fed antennas and rectennas.